Modeling collision avoidance maneuvers for micromobility vehicles

Journal of Safety Research xxx (xxxx) xxx

Contents lists available at ScienceDirect

Journal of Safety Research

journal homepage: www.elsevier.com/locate/jsr

Modeling collision avoidance maneuvers for micromobility vehicles

Tianyou Li *, Jordanka Kovaceva, Marco Dozza

The Department of Mechanics and Maritime Sciences at Chalmers University of Technology, Sweden

ARTICLE INFO

Article history:
Received 14 February 2023
Received in revised form 14 August 2023
Accepted 21 September 2023
Available online xxxx

Keywords:
E-scooters
Bicycles
Cycling safety
Micromobility vehicles
Active safety

ABSTRACT

Introduction: In recent years, as novel micromobility vehicles (MMVs) have hit the market and rapidly gained popularity, new challenges in road safety have also arisen. There is an urgent need for validated models that comprehensively describe the behavior of such novel MMVs. This study aims to compare the longitudinal and lateral control of bicycles and e-scooters in a collision-avoidance scenario from a top-down perspective, and to propose appropriate quantitative models for parameterizing and predicting the trajectories of the avoidance—braking and steering—maneuvers. *Method:* We compared a large e-scooter and a light e-scooter with a bicycle (in assisted and non-assisted modes) in field trials to determine whether these new vehicles have different maneuverability constraints when avoiding a rear-end collision by braking and/or steering. *Results:* Braking performance in terms of deceleration and jerk varies among the different types of vehicles; specifically, e-scooters are not as effective at braking as bicycles, but the large e-scooter demonstrated better braking performance than the light one. No statistically significant difference was observed in the steering performance of the vehicles. Bicycles were perceived as more stable, maneuverable, and safe than e-scooters. The study also presents arctangent kinematic models for braking and steering, which demonstrate better accuracy and informativeness than linear models. *Conclusions:* This study demonstrates that the new micromobility solutions have some maneuverability characteristics that differ significantly from those of bicycles, and even within their own kind. Steering could be a more efficient collision-avoidance strategy for MMVs than braking under certain circumstances, such as in a rear-end collision. More complicated modeling for MMV kinematics can be beneficial but needs validation. *Practical Applications:* The proposed arctangent models could be used in new advanced driving assistance systems to prevent crashes between cars and MMV users. Micromobility safety could be improved by educating MMV riders to adapt their behavior accordingly. Further, knowledge about the differences in maneuverability between e-scooters and bicycles could inform infrastructure design, and traffic regulations.

1. Introduction

According to the community database on crashes on European roads, there were 1,901 cyclist fatalities in 2020, and 1,880 in 2021, and this number has been stable for the last 10 years (European Road Safety Observatory Annual statistical report on road safety in the EU, 2021; 2022). In Sweden, 10,440 bicycle crashes were reported in the Swedish Traffic Accident Data Acquisition database during 2019 and 0.3% of the crashes resulted in fatalities (Fernández et al., 2022). Further, 30% of cyclist fatalities were in car-to-cyclist rear-end crashes (Fredriksson et al., 2014). Nowadays, new micromobility vehicles (MMVs) are becoming increasingly popular. The term MMV refers to all small vehicles that may share the road with automobiles: bicycles (pedal-powered and electrically assisted), electric kick scooters (e-scooters), Segway balance scooters, and forth. In this paper, for simplicity, we use "MMVs" to refer to the four types in our study, which are traditional bikes, electric bikes, public-sharing e-scooters, and personal e-scooters. These e-scooters, although used in similar situations as traditional bicycles, have novel designs, operation methods, and power sources (e.g., electricity-driven), which create different kinematics that must be understood for the safety of all road users (Billstein & Svernlöv, 2021; Dozza et al., 2022). Thus, to understand how e-scooters impact road safety and to develop countermeasures for reducing e-scooter accidents, it is essential to understand and quantify the behavior of their users.

Several studies on e-scooters have been conducted during the recent years. From a bottom-up perspective, García-Vallejo et al. (2020) and Klinger et al. (2021) studied the light personal e-scooter's dynamic behavior. Based on the benchmark bicycle

* Corresponding author at: Hörselgången 4, 417 56 Gothenburg, Sweden.
E-mail address: TIANYOU.LI@CHALMERS.SE (T. Li).

https://doi.org/10.1016/j.jsr.2023.09.019
0022-4375/

model, the former study claimed that e-scooters are completely unstable at all speeds, while the latter found self-stability for a certain range of speeds. Garman et al. (2020) designed a test course where eight participants maneuvered a light personal e-scooter on different surfaces with different foot positioning. The study produced valuable results in terms of the e-scooter's performance in straight riding, unexpected braking, slalom, and low speed turning, but also presented the difficulties in comparing the braking and steering performance across different e-scooter designs and rider expertise. Moreover, Vetturi et al. (2023) analyzed the kinematics of an e-scooter and an e-bike during braking with three participants and built a probabilistic mathematical model for estimating the braking distance of e-scooters and e-bikes and claimed that no significant differences were found between the two types of vehicles. In the study by Vella and Vigliani (2022) on three riders, the authors also found that road adherence, rider position, rider mass and experience might affect the e-scooters' longitudinal dynamics. These studies have helped us take the first step in understanding e-scooter safety, however, many of them conducted experiment over only a small group of population and modeled only the light personal e-scooters with simple linear models.

In our previous study (Dozza et al., 2023), we analyzed experiment data on the MMVs' longitudinal control (accelerating and braking) over a relatively larger group of 34 participants, but no public-sharing e-scooters were studied. In the work of Lee et al. (2020), slalom as the lateral control maneuver was studied, yet also only for the light personal e-scooters. The modeling of longitudinal kinematics also used a linear regression approach. In this study, we follow the procedure proposed by Dozza et al. (2022) for field data collection in order to model and compare not only longitudinal (braking) but also lateral (steering) control for bicycles (with and without assisted pedaling) and e-scooters. One popular model of public sharing e-scooters was also included in the comparison. In our field experiment, 36 participants performed braking and steering maneuvers on four MMVs in two emergency levels, in a rear-end collision avoidance scenario. Our main hypotheses were that: (1) compared with light personal e-scooters, the larger public-sharing e-scooters may have better braking performance; (2) steering performance across bicycles and e-scooters may not be significant different; and (3) braking and steering trajectories for all MMVs can be accurately predicted with simple arctangent models, which may bring better accuracy than the constant-acceleration model previously proposed. From a top-down perspective, this study examines these hypotheses and expands the exploration in e-scooter safety in a rear-end collision scenario, presenting additional results by comparing steering and braking (rather than just braking) and including different types of e-scooters (rather than just bicycles and personal light e-scooters).

2. Methods

The data collection and analyses in this study were adapted from the procedure of Dozza et al. (2022).

2.1. Participants

Thirteen female and 23 male subjects participated in this field-trial experiment on a test track by maneuvering a bicycle (with and without electrical support), a large e-scooter (L-Scooter, the model typically rented from e-scooter-sharing companies), and a light e-scooter (S-Scooter, the model typically purchased for personal use). The participants' mean age (±standard deviation) was 31.5 (±7.5) years, mean height (±standard deviation) was 1.74 (±0.11) m, and mean weight (±standard deviation) was 73.0 (±12.3) kg. Participants shorter than 1.60 m and heavier than 100 kg were excluded from the study to comply with each vehicle manufacturers' suggested height and weight. The inclusion criteria were that participants could ride a bicycle, were between 18 and 60 years old, had no disabilities, and had never been in a severe road crash. These criteria were set to control for possible biases in the results, as indicated by Dozza et al. (2022). The maneuvers required the participant to laterally and longitudinally control (e.g., accelerating, braking and steering) the vehicles in different conditions. Each subject signed a consent form before the experiment. The Swedish Ethical Review Authority (Etikprövningsmyndigheten) approved the study (Ref. 2022-00314-01). An ad-hoc health insurance covered the participants during the experiment.

2.2. Equipment

The S-Scooter (Ninebot ES2), L-Scooter (Voiager 5, based on Segway Max Plus X), and bicycle (MONARK Karin 3-VXL) were each equipped with a data logger and sensors to collect vehicle kinematics (Fig. 1). The MONARK bike was equipped with a front disc brake and a coaster brake in the rear, which is the traditional braking system in Sweden. As for the e-scooters, the S-Scooter was equipped with a front electric brake and a rear fender brake, while the L-Scooter had a front drum brake and a rear electric brake. Table 1 shows all the specifications of the vehicles used in this study. The data logger was based on a Raspberry Pi 3 model B, and kinematics were collected with an inertial measurement unit (IMU: PhidgetSpatial 3/3/3 1044_B, sampling rate 125 Hz). In addition, a light detection and ranging sensor (LIDAR: Hokuyo UXM 30LAH EWA, sampling rate 20 Hz), installed by the side of the test track before the cardboard car, was used to track the vehicles during the experiment. The signals were filtered using Savitzky-Golay filtering in MATLAB in the later steps.

A potentiometer was used to measure the steering angle for each vehicle (Fig. 1). A belt connecting the wheel mounted on the potentiometer and the handlebar transferred the changes in the steering angle as the handlebar rotated, varying the potentiometer's internal resistance. Then an analog to digital converter (ADC) was used to measure the voltage across the poles of the potentiometer, induced by such variation. A calibration recording was made to convert the voltage to steering angle. During the recording, the handlebar was gradually moved from $-30°$ to $30°$ in increments of $5°$, with $0°$ representing a straight handlebar position. A linear function with minimum squared error between the voltages and the corresponding angles was then derived from the data. This calibration was made for all the vehicles.

2.3. Protocol

All the participants were given time to get acquainted with the vehicles' operation, after which they were asked to brake and steer each of the three vehicles in four different collision-avoidance tasks. On average, the training phase before the experiment took 12 minutes per participant. A soft cardboard car ($2\ m \times 1\ m \times 0.5\ m$) placed at the end of the straight test track was the obstacle that the participants had to avoid. All four collision-avoidance tasks required the participants to bring the vehicle up to speed from a standstill and keep the speed above 15 km/h and as constant as possible. The current speed was visible, to the participant, on a display on the handlebar of the bike, e-bike, and the S-Scooter. For the L-scooter, a phone was attached to the handlebar, which showed the current speed from a GPS speedometer (paid mobile phone application). Two braking tasks required the participants to brake and fully stop the vehicle in front of the cardboard car, either comfortably (comfortable task) or harshly (harsh task). The other two tasks were steering tasks, which required the participants to steer away before crashing with the

Fig. 1. Instrumented vehicles with data loggers and inertial measurement units (IMUs). Panels A. and B. are adapted from our previous work (Dozza et al., 2022).

Table 1
Specifications of the vehicles used in the experiment.

	Bike	E-bike	S-Scooter	L-Scooter
Model	MONARK Karin 3-VXL		Segway Ninebot ES2	Segway Max Plus X
Weight [kg]	17.8	21.8	11.3	31.5
Power	N/A	250 W	300 W	400 W
		Front motor	Front motor	Rear motor
Drive mode	Pedaling	Front wheel assisted pedaling	Pure electric	Pure electric
			FWD	RWD
Max. speed [km/h]	N/A	25	25	25
Braking system	Front disc		Front electric	Front electric + drum
	Rear coaster		Rear fender	Rear electric + drum
Wheels	28″		8″ Front	11.5″ Front
	Pneumatic tires		7.5″ Rear	10″ Rear
			Solid rubber tires	Rubber + gel filled tires

cardboard car, either comfortably or harshly. In other words, in the comfort tasks, participants were asked to brake or steer comfortably. In the harsh tasks, the participants were asked to brake or steer as late and hard/fast as possible. For each participant, the order of the vehicles and tasks was randomized, although all tasks were completed for each vehicle before the participant rode the next. The experimental conditions are shown in Fig. 2. The bicycle was used both as an e-bicycle and a conventional bicycle by turning on or off the electrical assistance. Therefore, although only three vehicles were tested in this study, we present results for four different riding conditions: the light e-scooter, the large e-scooter, and the two bicycle configurations (assisted and non-assisted). In addition to the 16 primary tasks (4 vehicles × 4 tasks) that each participant performed, we also asked all of them to perform three repetitions of a task: (1) at the beginning (the first trial), (2) middle (the tenth trial), and (3) end (the nineteenth trial) of their experiment session. Seven participants repeated the comfortable braking maneuver riding the non-assisted bicycle and 10 participants riding the large e-scooter. Eleven participants repeated the comfortable steering maneuver riding the non-assisted bicycle and eight

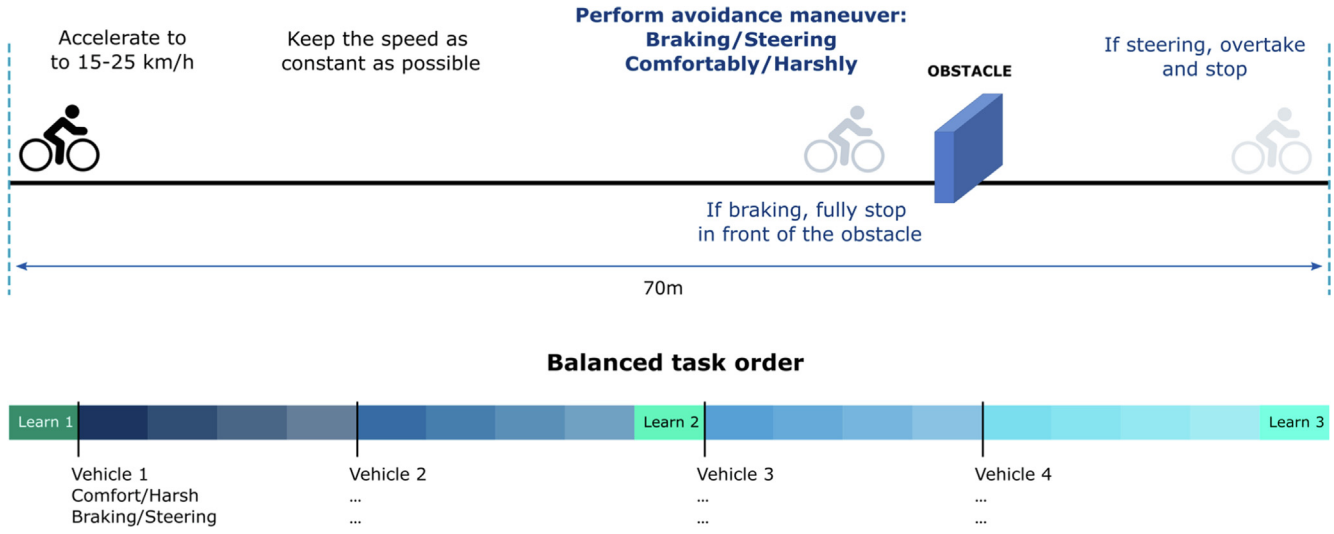

Fig. 2. Experimental protocol. For each vehicle, the four tasks: comfortable and harsh braking and steering, were shuffled for every participant. The 1st, 10th, and 19th trials, equal within each participant, were used to control for a learning effect.

participants riding the large e-scooter. These extra trials were used to investigate potential learning effects. These trials, comprising only the comfortable maneuvers on the non-assisted bicycle and the large e-scooter, were assigned randomly to each participant. In total, each participant performed 19 trials (Fig. 2, bottom).

2.4. Subjective data

The participants were asked to complete a questionnaire after completing all the tasks. The questionnaire requested: (1) their demographic data and how much previous experience they had with the different vehicles in the experiment, and (2) their opinions on the performance of the vehicles during the experiment. For part (2), adapted from previous works (Dozza et al., 2022), the participants ranked the four vehicles on a 7-level Likert scale (from 1 = Very poor to 7 = Exceptional). The following six performance categories were ranked: mounting and dismounting, maintaining balance, maintaining a constant speed, braking capability, steering capability, and accelerating from a standstill. The participants also scored each vehicle regarding its overall perceived comfort, maneuverability, stability, and safety using the same Likert scale.

2.5. Analyses

A DBSCAN clustering (Ester et al. 1996) over the LIDAR data were used to detect the rider, which resulted in a single cluster of points within a cuboid. The center of this cuboid was the representative of the combination of the rider-vehicle geometry. The speed of the central point was treated as the speed of the vehicle. The trajectories were calculated with the coordinates and the speeds (differentiation of distances) of the point.

The calculated trajectories were then used to model the braking and steering behavior for each vehicle. We used arctangent functions to fit the speed profile for the braking task and the avoiding maneuver's trajectory for the steering task. The coefficient R^2 was computed to verify the goodness of fit of the arctangent models. The distance covered to achieve a full stop was also computed for the braking maneuvers, which were defined as beginning when the vehicle deceleration exceeded 0.5 m/s^2 and as ending when the deceleration dropped below 0.5 m/s^2. In addition, for both the comfortable and harsh braking maneuvers, if the maximum braking jerk exceeded 20 m/s^3, the trial was removed. This jerk threshold was adapted from the vehicle research based on limits of driver comfort and vehicle systems (Brännström et al., 2010; Lubbe, 2017; Svärd et al., 2017). A steering maneuver was defined as beginning when the steering angle exceeded 5° while the lateral displacement (the distance between the center of the rider and the center of the cardboard car) exceeded 0.25 m, and as ending when the rider had overtaken the cardboard car (when the rear wheel of the vehicle passed the cardboard car). These thresholds were induced from our observations that the measurements would fluctuate or drift when the participants were riding straight. For each steering maneuver, a mean correction of the steering angle was made in order to correct for potential drift. The steering angle was assumed as zero during the period when the participants were riding straight and keeping the constant speed. The mean steer angle of the riding straight was therefore removed from the steer angle measurements for each maneuver. The data were then segmented based on the extracted braking and steering maneuvers, and the log times of the different sensors were synchronized. After the data segmentation, an arctangent fitting was performed on the longitudinal velocity profile for the braking maneuvers and the trajectory for the steering maneuvers. Four variables for the comfortable braking maneuver and four variables for the comfortable steering maneuver were extracted and analyzed in order to study the potential learning effect during the experiment (Table 2).

For the braking maneuver, the variables were the speed and longitudinal distance between the rider and the cardboard car when the participant started braking, the braking deceleration, and the final longitudinal distance (when the participant stopped). For the steering maneuver, the variables were the starting speed, the longitudinal distance when the participant started steering,

Table 2
The variables used in analysis of potential learning effect.

Comfortable braking	Comfortable steering
Speed when start braking	Speed when start steering
Longitudinal distance to the cardboard car when start braking	Longitudinal distance to the cardboard car when start steering
Maximum braking deceleration	Lateral distance to the cardboard car when start steering
Longitudinal distance to the cardboard car when stop braking	Lateral distance to the cardboard car when overtake it

and the lateral distances when the participant started steering, and when they overtook the cardboard car.

Several generalized linear mixed-effect (GLME) models (including the participant ID as a random effect and gender, vehicle type, and maneuver type as fixed factors) were created to verify the significance of the results. Post-hoc tests were run on the results of the model whenever a factor with more than two categories was significant. The threshold for statistical significance was set to $\alpha = 0.05$ and adjusted with the Bonferroni correction to control for multiple tests across different analyses with uncorrelated measures. (All statistical analyses used the Statistics and Machine Learning Toolbox in MATLAB, specifically the functions *fitglme* and *coefTest*.).

3. Results

3.1. Dataset

All 36 participants successfully completed all 19 tasks. Four participants crashed into the cardboard car when performing the harsh braking task on the light scooter, and two crashed when performing the harsh braking task on the large scooter. None of the participants crashed with the bicycles, nor did the participants crash when performing the steering tasks. The participants who crashed into the cardboard car were asked to try performing the same task again until they could brake and fully stop before hitting the cardboard car. Each trial with a crash was excluded from the analysis and replaced by a successful repetition of the same trial (when the participant did not crash). All participants except one were used to riding bicycles and/or electric bicycles and were less experienced with riding e-scooters (Table 3). Twenty out of 36 participants reported that they used helmets when riding bicycles and e-scooters.

For the L-Scooter, the average constant initial speeds that the participants achieved in both braking (Table 4) and steering (Table 5) maneuvers were statistically significantly higher than for the other three vehicles.

It is worth noting that no direct measurement for the vehicle speed (e.g., optical encoder for measuring the wheel speed) was used in our data collection. In addition, we experienced a significant data loss on all the on-vehicle IMUs due to a synchronization issue, mainly the consequence of malfunctioning time-synchronization modules in the IMUs. As a result, there were unknown time differences between the logger on the vehicles and the logger on LIDAR, requiring a large amount of work to manually synchronize them. Thus, in contrast with previous studies (Lee et al., 2020; Dozza et al., 2023; Dozza et al., 2022), the post-processing was based on the data collected from the LIDAR and potentiometers. Given the indirectness in the data collection, we were not able to measure the speed directly or compare the error in the speeds measured by different approaches (e.g., between LIDAR and IMU measurements).

3.2. Braking maneuvers

Fig. 3 shows the average longitudinal speeds across all subjects for comfortable and harsh braking maneuvers. Table 4 complements Fig. 3 by presenting the deceleration and jerk from the arctangent fitting models for all vehicles and maneuvers. In all maneuvers, the S-Scooter achieved lower deceleration and braking jerk than the other vehicles. Even though the L-Scooter achieved the largest deceleration in the comfortable braking maneuvers and the second largest in the harsh ones, there was no statistical significance in braking deceleration between the bicycle in assisted mode and the large e-scooter. Similarly, there was no statistically significant difference in braking jerk for the e-bike and the large e-scooter. The participants' braking performance when riding the S-Scooter was statistically significantly poorer (smaller decelerations) than the other vehicles. When riding the bicycle in assisted and non-assisted modes, the participants achieved similar braking deceleration and jerk. As expected, the harsh braking maneuver resulted in statistically significantly larger braking deceleration and jerk for all vehicles. What was somewhat surprising is that the average deceleration and jerk for the L-Scooter were the largest among all the vehicles in the comfortable braking task. No statistically significant effect of gender or age was found for braking deceleration or jerk.

Fig. 4 presents the braking distances of the four vehicles in comfortable and harsh braking maneuvers, which is defined as the distance traveled in between the moments when the rider started and stopped braking. As expected, the braking distances in the harsh maneuvers were significantly shorter than those in the comfort-

Table 3
Number of participants who have different levels of experience riding the various vehicles.

	Bike/E-Bike	E-Scooters
Never	1	10
Few days per year	9	11
Few days per month	9	10
Few days per week	9	4
Every day	8	1

Table 4
Average (M) braking acceleration (m/s^2), jerk (m/s^3), and initial speed (km/h) when the participants started to brake with standard deviations (SD). N indicates the number of trials available for computing averages and standard deviations. We also report the average R^2 coefficients to show the goodness of fitness of arctangent models.

			Bicycle	E-Bicycle	S-Scooter	L-Scooter
Comfort	Number of samples (N)		35	36	35	35
	Acceleration	M ± SD	−1.66 ± 0.68	−1.69 ± 0.55	−1.65 ± 0.56	−1.98 ± 0.59
	[m/s^2]	R^2	0.97	0.97	0.99	0.99
	Jerk	M ± SD	−1.19 ± 1.64	−0.99 ± 0.80	−0.98 ± 0.91	−1.15 ± 0.84
	[m/s^3]					
	Initial speed	M ± SD	18.81 ± 2.31	20.51 ± 2.50	20.03 ± 2.31	23.40 ± 2.49
	[km/h]					
Harsh	Number of samples (N)		28	34	34	33
	Acceleration	M ± SD	−3.93 ± 1.55	−4.24 ± 1.69	−2.92 ± 1.00	−4.04 ± 1.24
	[m/s^2]	R^2	0.97	0.98	0.98	0.99
	Jerk	M ± SD	−6.22 ± 4.74	−6.83 ± 5.60	−3.17 ± 2.69	−4.97 ± 3.30
	[m/s^3]					
	Initial speed	M ± SD	18.93 ± 2.21	20.31 ± 1.42	19.95 ± 2.61	23.54 ± 2.48
	[km/h]					

Table 5
Average (M) lateral offset (m) when the participants overtook the cardboard car and maximum steering angle (degree), with standard deviations (SD), and initial speeds (km/h). N indicates the number of trials available for computing averages and standard deviations. We also report the average R^2 coefficients to show the goodness of fitness of arctangent models. Number of samples (N) always equals 36.

			Bicycle	E-Bicycle	S-Scooter	L-Scooter
Comfort	Lateral offset [m]	M ± SD	2.80 ± 0.84	2.81 ± 0.82	2.73 ± 0.75	2.73 ± 0.86
		R^2	0.99	0.99	0.99	0.99
	Steer angle Max. [°]	M ± SD	30.72 ± 16.05	29.64 ± 12.83	32.58 ± 14.53	32.10 ± 18.71
	Initial speed [km/h]	M ± SD	15.81 ± 4.72	17.07 ± 4.62	19.95 ± 5.13	18.69 ± 4.24
Harsh	Lateral offset [m]	M ± SD	1.94 ± 1.06	1.97 ± 0.93	2.10 ± 0.90	2.11 ± 0.90
		R^2	0.98	0.99	0.99	0.99
	Steer angle Max. [°]	M ± SD	30.37 ± 12.89	29.44 ± 13.11	33.64 ± 22.03	32.93 ± 16.75
	Initial speed [km/h]	M ± SD	17.76 ± 5.49	17.65 ± 5.29	21.50 ± 4.95	19.97 ± 3.64

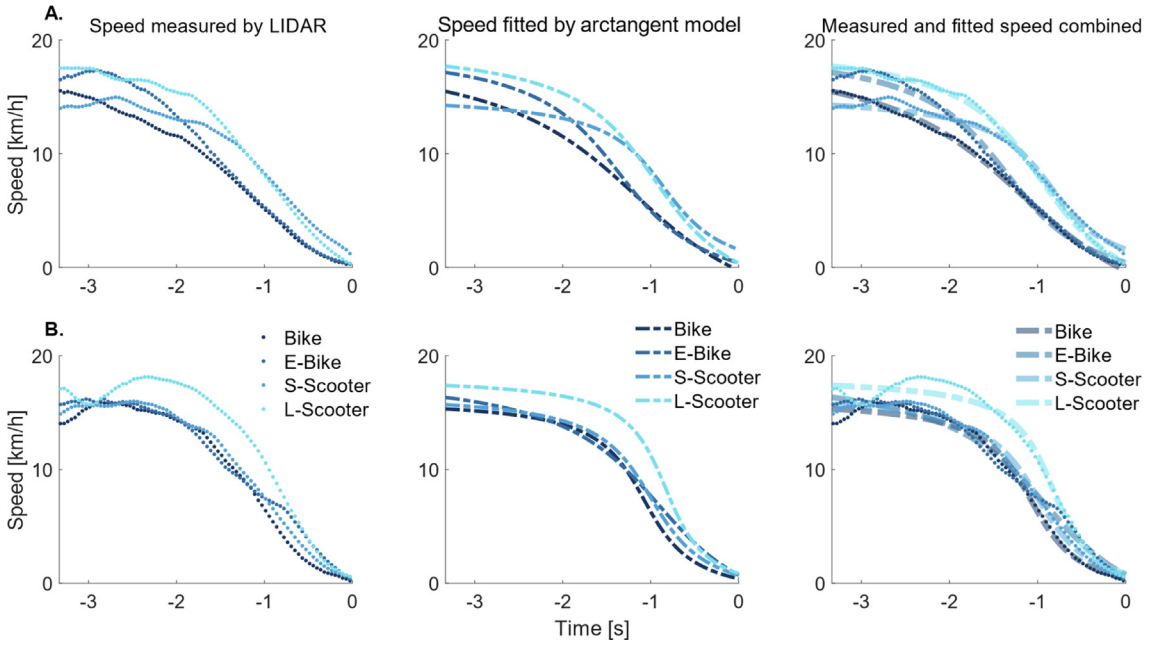

Fig. 3. Average speed for comfort (row A) and harsh (row B) braking maneuvers for all vehicles. Dotted lines are the measures of velocity. Dashed lines are the arctangent fittings of the average longitudinal speed. In each row there are 3 columns showing the speed measured by LIDAR, fitted by arctangent model and the combination of the former two.

able maneuvers across all the vehicles. In both comfortable and harsh maneuvers, while the braking distance for the non-assisted bicycle was slightly longer than that for the assisted bicycle, the distances for the bicycle in both modes were statistically significantly shorter than the distances for the two e-scooters, especially in the harsh braking maneuvers. As expected, both deceleration and jerk were statistically significantly greater (Table 4) in the harsh maneuvers than in the comfortable maneuvers, and the two e-scooters achieved statistically significantly less jerk than the bicycles in the harsh maneuvers. Since the initial speed of the vehicles varied, the comparison between braking distances may be more meaningful when distinguishing comfortable and harsh maneuvers within one specific vehicle, than across vehicles. The braking performance across different vehicles are mainly indicated by the statistical results in the tables in the Appendix.

In addition, a slight lateral displacement (0.54 ± 0.47 m, in average) was observed during the braking maneuvers for all vehicles. This suggests that the participants tended to steer away from the cardboard car in front of them in the braking tasks, even when they had been asked to keep riding in a straight line.

3.3. Steering maneuvers

The average lateral offsets over time for the two steering maneuvers are presented in Fig. 5. In addition, Table 5 reports the participants' average lateral offset when they overtook (when their rear wheel passed) the cardboard car and their maximum steering angle. Harsh maneuvers resulted in statistically significantly smaller lateral offsets than comfortable maneuvers, indicating that the participants understood the instructions and steered the vehicles away as late as possible. No statistically significant difference in lateral offset was found across ages or genders. The participants achieved similar lateral offsets when riding the two e-scooters in comfortable braking maneuvers. The bicycle achieved statistically significantly larger lateral offsets in assisted mode than in non-assisted mode, and no statistically significant difference

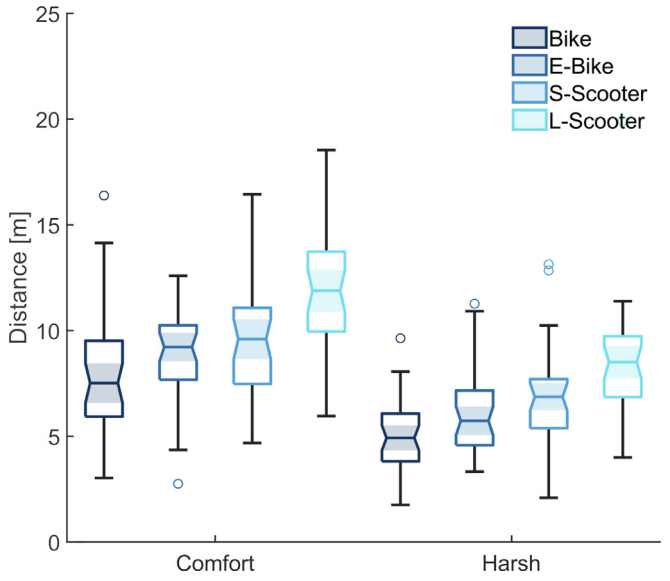

Fig. 4. Braking distances of the four vehicles in comfortable and harsh braking maneuvers. Circles indicate outliers, whiskers are set by the non-outlier minima and maxima of the distribution, and the central horizontal line represents the median, while the horizontal edges of the box are the 25th and 75th percentiles. The notches, highlighted with shading, indicate the confidence intervals. (These boxplots were generated with the boxchart command in MATLAB.)

was observed between other vehicles. Finally, in both comfortable and harsh steering maneuvers, there was no statistically significant difference in the maximum steering angle for the four vehicles. A change in speed (−0.88 ± 0.92 m/s) which was statistically significantly larger for both e-scooters was observed in the steering maneuvers. In essence, even though the participants were asked to keep a constant speed, they still slowed down during steering.

3.4. Learning

Seventeen participants repeated the comfortable braking maneuver, 7 riding the non-assisted bicycle and 10 riding the large e-scooter. Of the four variables analyzed, only the longitudinal distances between the rider and the cardboard car when the participants stopped showed a potential learning effect. For the non-assisted bicycle, the final distance decreased as the experiment progressed. In contrast, for the large e-scooter, the distance increased. Both results were statistically significant.

Nineteen participants repeated the comfortable steering maneuver, 11 riding the non-assisted bicycle and 8 riding the large e-scooter. No trend or statistically significant difference was found in the four variables we tested.

3.5. Arctangent model

Braking jerk is a crucial variable for safety because it can be used in optimal trajectory planning (Viviani & Flash, 1995), vehicle threat assessment (Biral et al., 2012), and aggressive driver identification (Feng et al., 2017), among other applications. By fitting the vehicle speed with an arctangent model, we were able to efficiently derive the longitudinal deceleration and jerk during the braking maneuvers. Fig. 6 shows one example of using the arctangent function to fit the vehicle speed for a comfortable braking maneuver on a non-assisted bicycle.

As the R^2 value shows in Tables 3 and 4, the arctangent function results in a highly accurate fit of the longitudinal speed and lateral offset. The arctangent fitting requires four coefficients to converge, denoted in Equation (1).

$$y = a \cdot \arctan(b \cdot t + c) + d \tag{1}$$

Table 6 shows the four coefficients (M ± SD) for the average arctangent model of a comfortable braking maneuver on the e-bike. These coefficients will be discussed in detail in the Discussion section. As for the steering maneuvers, a similar process could be applied to study lateral speed, deceleration, and jerk.

The four coefficients of the arctangent model (Eq. (1)) could also be interpreted. Coefficient a can be used to approximate how much the measured value has changed (the scale of the y-axis). For the braking and steering maneuvers, one can estimate the initial speed before braking and the lateral offset when overtaking the obstacle by:

$$\Delta y = a \cdot \pi \approx 2 \cdot d(y_{initial/final} = 0) \tag{2}$$

If the initial/final value is zero (steer away from obstacle center/brake from initial speed to zero), Eq. (2) then approximates $2 \cdot d$ (see also Eq. (5)).

Similarly, the coefficient b indicates the change rate of the measured value (the scale of the x-axis). In our case, when the x-axis represents time, the larger the absolute value of the coefficient b is, the faster the measured value (e.g., vehicle speed, lateral offset) changes. With coefficient a, one can estimate the minimum deceleration using Eq. (3).

$$deceleration_{min} = a \cdot b \tag{3}$$

One can also easily calculate the minimum jerk with Eq. (4).

$$Jerk_{min} = -\frac{3\sqrt{3}}{8} \cdot \left| a \cdot b^2 \right| \tag{4}$$

Note that for a descending signal (e.g., vehicle speed when braking), a and b should have opposite signs. When the x-axis represents time, a larger coefficient c indicates an earlier change to the measured value, and vice versa. Table 7 shows how the initial speed, deceleration, jerk, and duration of the maneuver are calculated with the coefficients. Since b and c determine the zero point of the arctangent function, they are highly covaried. In our study, for the events that happen after zero-time, b and c should always have opposite signs, while a and c should have the same signs when the measured value decreases and opposite signs when it increases (e.g., speed in acceleration, and lateral offset when steering to the left). Finally, coefficient d can be used to estimate the initial or final measured value using Eq. (5).

$$y_{initial/final} = d - \frac{a \cdot \pi}{2} \tag{5}$$

Alternatively, if an MMV's deceleration and/or jerk performance parameters are known, one can quickly approximate the trajectory of the MMV for the threat assessment by computing the required deceleration or jerk with Eqs. (2)–(4).

3.6. Subjective data

Table 8 shows some of the participants' opinions of the vehicles' performance in different situations. The electrified vehicles, possibly because they required less physical effort, were perceived as more comfortable than the non-assisted bicycle when accelerating from a standstill, and this result was statistically significant. The assisted and non-assisted bicycle tasks scored similarly in all other situations (without statistically significant differences). Compared to both bicycle modes, the two e-scooters scored statistically significantly lower for turning, maintaining balance, and steering, and higher for maintaining a constant speed. There is no statistically significantly difference in the score of braking between the

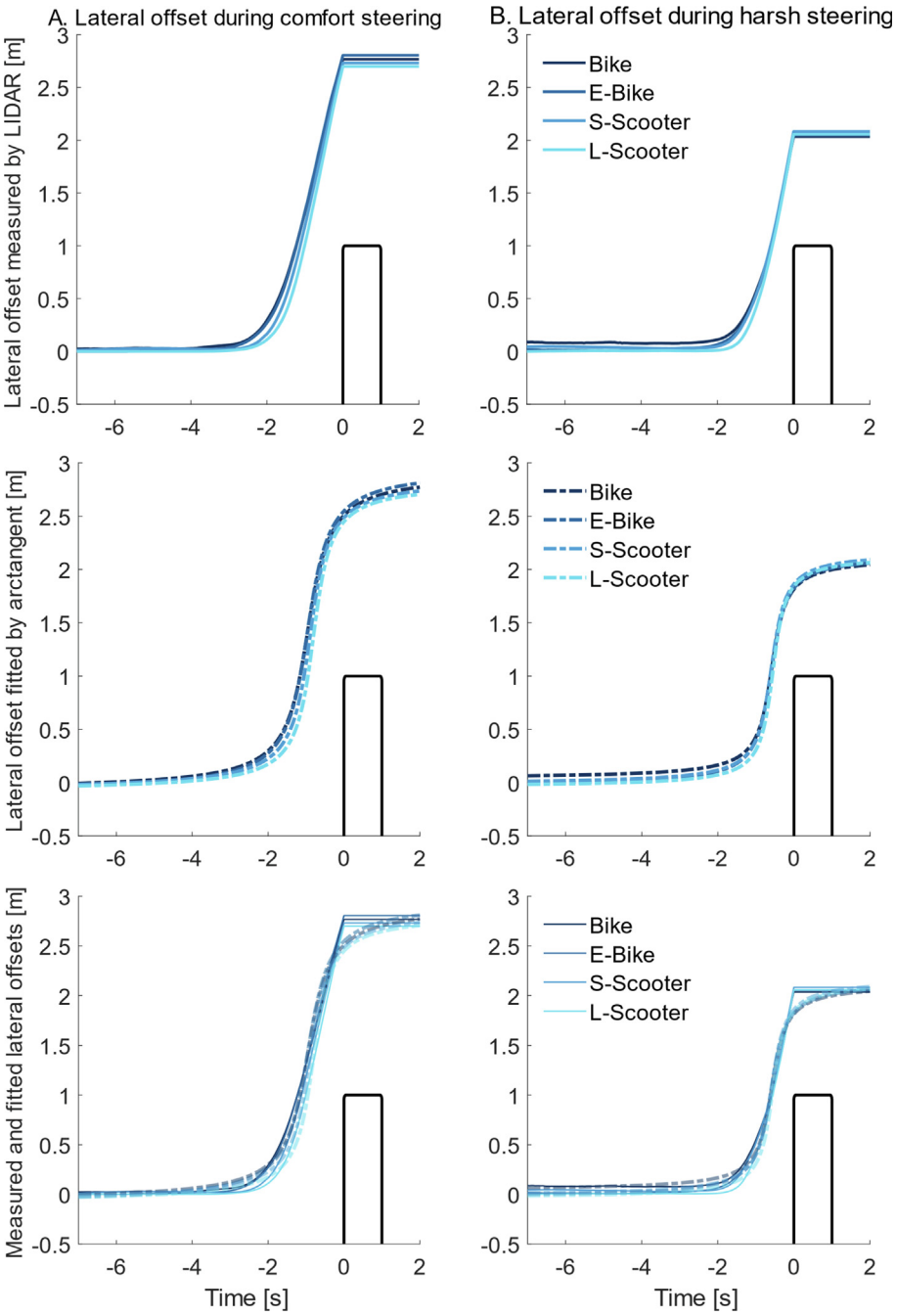

Fig. 5. Average lateral offset for comfort (column A) and harsh (column B) steering maneuvers for all vehicles. Dashed lines are the arctangent fittings of the average lateral offset. The rectangle at the right bottom shows the lateral position of the cardboard car.

L-Scooter and the bicycles, however the S-Scooter was still scored the statistically significantly lowest score for braking. Among the two e-scooters, the L-Scooter scored statistically significantly higher than the S-Scooter in all categories, and these results were statistically significant. The statistical results for "Braking" and "Steering" from the GLME analysis are presented in the Appendix.

4. Discussion

In this study, we applied the procedure for data collection and analysis presented in Dozza et al.'s 2022 field study to the comparison of the longitudinal and lateral control of a bicycle (with and without assisted pedaling), a light personal e-scooter, and a large public sharing e-scooter. Our results show that the same participant may demonstrate different braking and steering performances depending on the vehicle and the urgency. Nevertheless, we also verified that, independently of the vehicle and the urgency of the maneuver, riders braked with variable decelerations and jerks, and steered with variable steering angles and lateral clearances. Steering could be safer than braking for e-scooter riders in collision avoidance because of the poor braking performance that e-scooters demonstrated.

As for braking, the participants could brake almost twice as harshly when they braked harshly, as per instructions. This is in accordance with our previous study (Dozza et al., 2022). The result

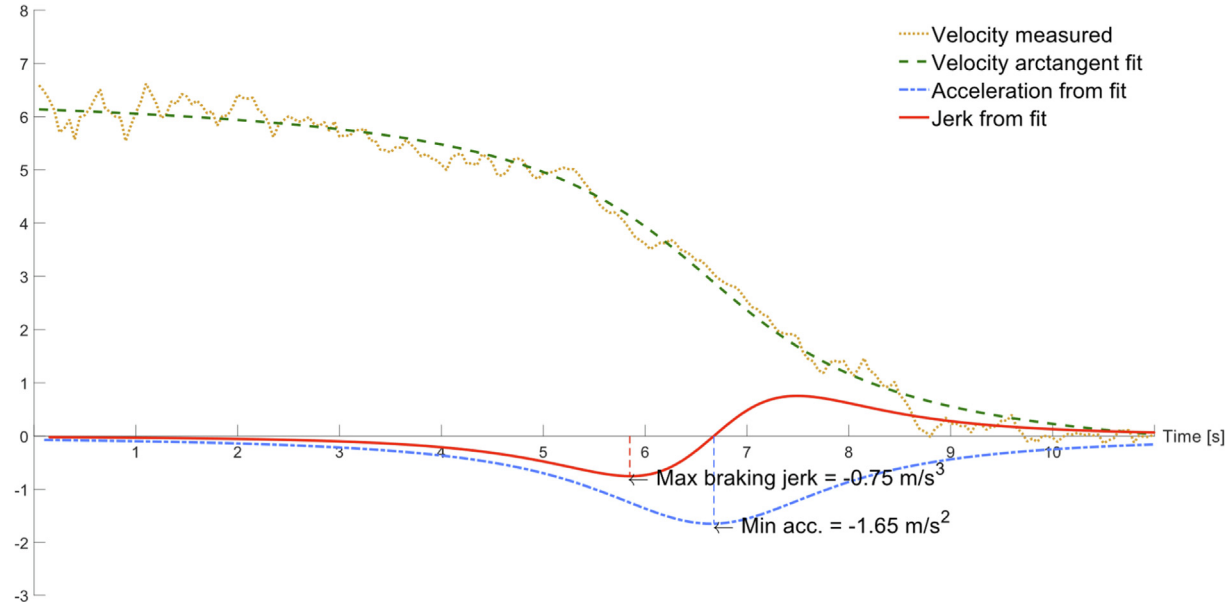

Fig. 6. An example of using the arctangent function to fit the longitudinal speed for a braking maneuver.

Table 6
Coefficients for arctangent model (a_a, b_a, c_a, d_a) compared to the linear model ($y = a_l \cdot t + b_l$) in average comfortable braking maneuvers when riding the assisted bicycle. Speed, deceleration, and jerk are calculated in m/s, m/s^2, and m/s^3, respectively. Duration indicates the time in seconds from starting braking to stopping completely.

Arctangent model				Linear model
1.18 ± 0.54	a_a	Coefficient 1 (a)	a_l	−1.80 ± 0.31
−0.80 ± 0.37	b_a	Coefficient 2 (b)	b_l	5.70 ± 2.50
1.90 ± 1.04	c_a	Coefficient 3 (c)	N/A	-
2.83 ± 0.31	d_a	Coefficient 4 (d)	N/A	-

Table 7
Comparison between coefficients of the arctangent model and linear model. Kinematic parameters are calculated with the coefficients and their combinations.

Arctangent model				Linear model
−1.69 ± 0.55	$a_a \cdot b_a$	Min. acceleration [m/s^2]	a_a	−1.80 ± 0.31
5.66 ± 0.62	$2 \cdot d_a$	Initial speed [m/s]	b_a	5.70 ± 2.50
−0.99 ± 0.80	$-3\sqrt{3}/8 \cdot \lvert a_a \cdot {b_a}^2 \rvert$	Min. jerk [m/s^3]	N/A	-
4.79 ± 1.42	$-2 \cdot c_a/b_a$	Duration [s]	$-b_a/a_a$	3.25 ± 0.63

Table 8
Average values and ranges of the subjective data for all vehicles (from 1 = Very poor to 7 = Exceptional).

	Bike	E-Bike	S-Scooter	L-Scooter
Accelerating from standstill	3.75 (1–6)	5.06 (2–7)	4.36 (2–7)	5.14 (3–7)
Turning (large angles)	4.94 (3–7)	4.81 (2–7)	3.81 (2–6)	4.33 (2–6)
Maintaining balance	5.33 (3–7)	5.36 (3–7)	4.11 (1–7)	4.61 (3–7)
Maintaining a constant speed	4.39 (2–7)	4.47 (2–7)	4.86 (2–7)	5.11 (4–7)
Braking	5.08 (3–7)	5.06 (3–7)	2.94 (1–6)	4.83 (2–7)
Steering	5.14 (3–7)	5.09 (2–7)	3.56 (2–6)	4.25 (3–7)
Overall comfort	4.64 (1–6)	4.94 (2–7)	3.22 (1–6)	4.83 (3–6)
Overall maneuverability	5.06 (2–7)	4.97 (2–7)	3.61 (1–6)	4.64 (3–6)
Overall stability	5.36 (2–7)	5.42 (3–7)	3.39 (1–6)	4.64 (3–7)
Overall safety	5.28 (3–7)	5.11 (3–7)	3.22 (1–6)	4.31 (2–7)

also match the one presented in the study by Vella and Vigliani (2022), where the authors collected deceleration data generated by three riders braking a light e-scooter on two different road surfaces and three emergency levels. What was surprising in the braking maneuvers was that there was no statistically significant difference in the deceleration and jerk between the L-Scooter and the bicycles. This may be a consequence of the statistically significantly higher speed achieved by the participants when riding the L-Scooter before they started braking. However, even though the average initial speeds of the e-scooters were higher than the bicy-

cles, we can still draw the conclusion that the L-Scooter demonstrated a statistically significantly poorer braking capacity than the bicycles. This conclusion is reached by considering the e-scooter's statistically significantly higher initial speed and statistically insignificantly different deceleration comparing with the bicycles' (Appendix). Similarly, we can see that the L-Scooter demonstrated a statistically significantly better braking capacity than the small personal e-scooter. The standard deviations of the speed for all vehicles were also small (less than 2.6 km/h, Table 3). In the previous study by Vetturi et al. (2023), where the authors also used an indirect approach (camera image processing) for measuring the vehicles' kinematics, the braking maneuver was modeled with linear regression models and constant accelerations. The authors claimed that there was no significant difference in the maximum braking decelerations between e-bikes and e-scooters. However, our results have shown that even though the large public-sharing e-scooter achieved maximum braking decelerations similar to e-bikes, the light personal e-scooters still demonstrated statistically significantly poorer braking capacity. The results above have validated our first hypothesis, that the larger public sharing e-scooter performs better in braking. However, the braking performance of the L-Scooter is still poorer than the bicycles.

In the steering maneuvers, the riders steered away at almost the same angles in both comfortable and harsh steering maneuvers. However, the lateral distances they traveled were statistically significantly smaller in the harsh maneuvers, which indicates that the lateral clearance would decrease as the urgency increased. Since the measurements of steering angle were affected by higher noise level, we consider the maximum lateral offset as a main indicator for analyzing the steering performance. The maximum lateral offsets did not show statistically significantly difference across all the vehicles (Appendix). Similar to braking, the initial speeds of the e-scooters were higher than the bicycles. However, this uncertainty can be mitigated by also considering the results from the GLME analysis, that the e-scooters demonstrated statistically significantly higher initial speeds than bicycles, yet the maximum lateral offsets as well as the durations of the steering maneuver showed no statistically significant difference across all the vehicles. It is worth noting that unlike the arctangent model's results for braking, which predicted larger safety margins than the linear model (i.e., smaller decelerations and longer braking durations; Table 6), the same model's fit of the lateral offset for steering maneuvers resulted in earlier "saturation" (i.e., the fitted arctangent curve steered back earlier than the riders did; Fig. 5). Even though the goodness of fit was high, this difference could result in false negatives in the threat assessment, since the actual required lateral clearance for the riders to comfortably steer is larger than the one predicted by the model. This error could be reduced once the IMU data are accessible so that more kinematic information about the vehicles can be used for reconstructing the trajectories and improving the modeling. Moreover, even the e-scooters had poor braking capabilities compared to the bicycle in either mode, while they did not show statistically significant differences in the steering measures. Thus, in some scenarios, it may be a better strategy for e-scooter riders to avoid a collision by steering away instead of braking. The decision by riders to brake or steer in e-scooters and other micromobility vehicles could also be modeled similarly as Brännström et al. (2010) did for the decision-making of threat assessment in car ADAS, which based on the driver's comfort limits and the vehicle system's limits. These results partially favor our second hypothesis that the steering maneuver on bicycles and e-scooters are similar.

When we investigated the potential learning effect during the experiment, we found that only one parameter, the longitudinal distance to the cardboard car when the participants stopped braking, statistically significantly changed (shorter for the non-assisted bicycle and longer for the large e-scooter) as the participants progressed in the experiment. However, this is not solid evidence of learning because the dataset may have been very small in both sample size and time span. Due to the technical error, it was not possible to fuse the data from the IMUs, thus the decelerations and jerks (computed from the LIDAR data) may introduce some errors and uncertainty. However, by looking at the deceleration and jerk curves, we noticed that both quantities took longer to increase than those achievable for cars, which means a constant deceleration model (a constant-deceleration linear model), or a constant jerk model may not accurately model micromobility vehicles' kinematics.

In this study, we proposed an arctangent model for analyzing MMV kinematics. Compared with the linear regression model used in our previous work (Lee et al., 2020; Dozza et al., 2022), the arctangent model has the following advantages: it (1) provides more information about jerk, (2) increases the safety margin by accounting for the buildup of deceleration and jerk, and (3) describes the rider trajectories more smoothly and naturally, as the four coefficients can be directly used to approximate various kinematical parameters rapidly. However, there are also limitations of the arctangent model: it is (1) less computationally efficient, (2) more conservative (and could issue false positives), and (3) unable to describe the asymmetry in the braking jerk and deceleration, that according to, Wada et al. (2010) a driver/rider would apply the brake faster than they release it. The results from the analysis support our third hypothesis that an arctangent model could be a better fit for modeling low-speed MMVs. However, direct measurements of the kinematic parameters should be compared in future work to further validate this hypothesis.

Even though the deceleration, jerk, and lateral offset may change depending on the urgency of the maneuvers and the vehicle type, it is still possible for active safety systems to predict rider trajectories, thanks to the constancy in the arctangent-like braking and steering patterns. The systems may be able to estimate the probability that, for example, a rider ahead who is trying to avoid a rear-end collision can overtake or stop in front of the obstacle in time-and use this information to issue warnings to the driver or apply automated interventions (such as emergency braking and steering). The L-Scooter in this study is representative of the e-scooters that are available in sharing programs, and the S-Scooter is typical of those that can be purchased for personal use in Sweden. These two types of e-scooters have many differences, such as battery capacity, weight, steering torque, suspension, wheel size, and brakes. Future studies should further compare different e-scooter models to determine whether any of these differences affect riding safety. For instance, the electric braking system of the e-scooters used in this study may result in longer braking distances compared to the bicycle (assisted and non-assisted). E-scooter sharing programs have developed rapidly in recent years, and the e-scooters they use have also been evolving in terms of safety. The L-Scooter in this study, representing the latest generation of shared e-scooters, showed a strong similarity to a bicycle in its braking appearance, front suspension, and size; as a result, the participants took less time to learn how to use it than they took for the light personal e-scooter, which has no handbrake. In addition to the higher speed that the e-scooter could reach, one other reason why the L-Scooter had the statistically significantly longer braking distance and a lower subjective score than the bicycle's two modes in the "braking" category might be the participants' misperception of the vehicle's brakes. They might have expected the braking capability of a bicycle, simply because the two braking systems looked alike, even though the information on the brakes was given to them before the training phase. Similarly, as shown in Table 8, the e-scooters also scored statistically significantly

lower in many other categories, such as overall maneuverability and stability-especially in turning (larger angles) and steering. These differences might be a consequence of the participants' inexperience in using body lean to steer the vehicles, rather than the handlebar. Thus, more education about operating, not only e-scooters, but other new micromobility vehicles, is still needed.

This study still encounters several limitations. First of all, our sample of 36 participants may not be representative of all geographical locations and ages. In addition, the controlled field experiment may not be realistic as we excluded other road users and scenarios. Moreover, when riding the non-assisted bicycle, the rider had to carry the weight of the battery, since we used the same bicycle for the electrically assisted trials. Regarding the analysis, the initial speeds that the participants kept when they started braking or steering differed. The electric assisted/driven vehicles used in the experiment had a speed limit of 25 km/h while the participants were only asked to bring up and keep a constant speed above 15 km/h. Not controlling the initial speed may decrease the accuracy and validity of the comparison of braking performance across different vehicles, due to the potential effect that the parameter may have on the indicators for braking performance such as braking distance and acceleration. Furthermore, the errors and limitations introduced by the indirect approach for measuring vehicles' kinematics in the data collection and analysis was not addressed. Specifically, the velocity, acceleration, and jerk were calculated by differentiating the position data measured from a LIDAR with a relatively low sampling rate (20 Hz), which approximated the vehicle-rider system as a central point of a cluster of points. Future work, to improve the accuracy of the models, should include more direct measurements (e.g., wheel speed measurements using optical encoder with higher sampling rate) to be compared with the LIDAR measurements.

5. Conclusions

This study collected and analyzed field data on bike and e-scooter riders' collision avoidance behaviors. The field data demonstrates that each of the MMVs impacts riders' behavior in different ways, posing different challenges for controlling the vehicle. Braking and steering maneuvers were studied through field experiment. The experiment has shown that the large public sharing e-scooters perform better than the smaller personal e-scooters, especially in the braking maneuver. In addition, steering maneuvers across all the vehicles were proven to be similar. Finally, an arctangent model was proposed to replace the linear regression model for better modeling and predicting MMV kinematics. By modeling MMV kinematics, we can improve the threat assessment of advanced driver assistance systems (ADAS) and promote a better understanding of how e-scooters differ from bicycles from a safety point of view. Although the descriptive mathematical models for the e-scooter control are the focus of our study, the results presented in this paper may inform policy making, education on MMVs, and infrastructure design. Future studies should compare additional MMV models in different interactive traffic scenarios among a larger and more diverse sample of participants to obtain a deeper understanding of MMV kinematics thus to improve the safety.

An arctangent fitting model was proposed and demonstrated satisfactory goodness of fit for both braking and steering maneuvers. The coefficients from the arctangent model could be used to efficiently compute the maximum acceleration/deceleration and jerk achieved by a rider, as well as the required deceleration and jerk in a threat assessment system. In contrast with linear regression models, the arctangent model can provide information on other kinematic parameters, such as the jerk, beyond velocity and acceleration; the model can also predict or generate MMVs' trajectories in a more accurate, natural, and smooth manner. In certain scenarios, steering as an alternative option in rear-end collision avoidance is less constrained by the type of MMV than braking, and could be a better choice for those e-scooters with poorer braking capabilities than traditional bicycles. Future studies could focus on including other constraints and scenarios in the steering test, such as an oncoming vehicle in the riders' path as they veer away while overtaking.

The market for publicly shared e-scooters has been pushed to offer new e-scooters that are safer, heavier, and more robust and intelligent. Even though the L-Scooter braked better than the S-Scooter in the trials, we should not ignore the possibility that its evolution may have also brought new challenges, such as rider's misperception of and overconfidence in the vehicle (e.g., riders may expect a braking capability that is too high for the large e-scooter's handbrakes because they look more similar like bicycle handbrakes, and they can use them more intuitively). Sufficient education and tailored regulations are necessary to enhance the safety of e-scooter users.

ADAS, specifically automated emergency braking and steering, should take advantage of the models from this study in their threat assessments. When vehicle drivers and MMV riders share the road (as is common in many European cities), sometimes the rider needs to enter the safety margin between them. For example, they may want to avoid a suddenly appearing obstacle, or brake harshly when turning their attention back to the road after having been distracted. In such scenarios, an ADAS should be able to issue warnings or intervene. Results of this study can be also utilized to create appropriate test scenarios for consumer rating programs such as Euro NCAP. As indicated by the arctangent models for both comfortable and harsh maneuvers, riders took some time to reach maximum braking and steering capacity. Thus, current threat assessment models that use a constant or linear model for the deceleration and lateral offset may be inaccurate (and therefore less safe) since they assume the braking/steering maneuvers take effect instantly. The models presented in the paper are beneficial for helping vehicle systems predict the control abilities that MMV users have. Further research is necessary to determine whether jerk is an appropriate parameter for modeling MMV rider behavior and influencing threat assessment system engineering; it is already utilized in analyzing and predicting driver and motorcycle rider behavior. Future studies should also focus on better models for e-scooter kinematics and the rider, both as two separate entities and as an interconnected system.

Declaration of Competing Interest

The authors declare that they have no known competing financial interests or personal relationships that could have appeared to influence the work reported in this paper.

Acknowledgments

The data collection, analyses, and modeling effort were sponsored by Toyota Motor Europe via the DICE project (driver interaction with cyclists and e-scooterists at intersections) and Chalmers. The work was carried out at Chalmers University of Technology, Gothenburg, Sweden.

We also acknowledge the contribution from Shin Tanaka at Toyota Motor Corporation in Japan, who co-supervised the modeling effort.

Appendix A. Supplementary material

Supplementary material to this article can be found online at https://doi.org/10.1016/j.jsr.2023.09.019.

References

Billstein, L., & Svernlöv, C. (2021). Evaluating the Safety and Performance of Electric Micro-Mobility Vehicles: Comparing E-bike, E-scooter and Segway based on Objective and Subjective Data from a Field Experiment.

Biral, F., Lot, R., Rota, S., Fontana, M., & Huth, V. (2012). Intersection support system for powered two-wheeled vehicles: Threat assessment based on a receding horizon approach. *IEEE Transactions on Intelligent Transportation Systems, 13*(2), 805–816.

Brännström, M., Coelingh, E., & Sjöberg, J. (2010). Model-based threat assessment for avoiding arbitrary vehicle collisions. *IEEE Transactions on Intelligent Transportation Systems, 11*(3), 658–669.

Dozza, M., Li, T., Billstein, L., Svernlöv, C., & Rasch, A. (2023). How do different micro-mobility vehicles affect longitudinal control? Results from a field experiment. *Journal of Safety Research*.

Dozza, M., Violin, A., & Rasch, A. (2022). A data-driven framework for the safe integration of micro-mobility into the transport system: Comparing bicycles and e-scooters in field trials. *Journal of Safety Research, 81*, 67–77.

Ester, M., Kriegel, H. P., Sander, J., Xu, X., et al. (1996). A density-based algorithm for discovering clusters in large spatial databases with noise. *Kdd, 96*, 226–231.

Euro NCAP TEST PROTOCOL – AEB/LSS VRU systems, 2021.

European Road Safety Observatory Annual statistical report on road safety in the EU 2022.

Feng, F., Bao, S., Sayer, J. R., Flannagan, C., Manser, M., & Wunderlich, R. (2017). Can vehicle longitudinal jerk be used to identify aggressive drivers? An examination using naturalistic driving data. *Accident Analysis & Prevention, 104*, 125–136.

Fernández, P. D., Lindman, M., Isaksson-Hellman, I., Jeppsson, H., & Kovaceva, J. (2022). Description of same-direction car-to-bicycle crash scenarios using real-world data from Sweden, Germany, and a global crash database. *Accident Analysis & Prevention, 168* 106587.

Fredriksson, R., Fredriksson, K., & Strandroth, J. (2014). Pre-crash motion and conditions of bicyclist-to-car crashes in Sweden. In: International Cycling Safety Conference (p. 4).

García-Vallejo, D., Schiehlen, W., & García-Agúndez, A. (2020). Dynamics, control and stability of motion of electric scooters. In *Advances in dynamics of vehicles on roads and tracks: Proceedings of the 26th symposium of the international association of vehicle system dynamics, IAVSD 2019, August 12–16, 2019, Gothenburg, Sweden* (pp. 1199-1209). Springer International Publishing.

Garman, C. M., Como, S. G., Campbell, I. C., Wishart, J., O'Brien, K., & McLean, S. (2020). *Micro-mobility vehicle dynamics and rider kinematics during electric scooter riding* (No. 2020-01-0935). SAE Technical Paper.

Klinger, F., Klinger, M., Edelmann, J., & Plöchl, M. (2022). Electric scooter dynamics-from a vehicle safety perspective. In *Advances in dynamics of vehicles on roads and tracks II: Proceedings of the 27th symposium of the international association of vehicle system dynamics, IAVSD 2021, August 17-19, 2021, Saint Petersburg, Russia* (pp. 1102–1112). Cham: Springer International Publishing.

Lee, O., Rasch, A., Schwab, A. L., & Dozza, M. (2020). Modeling cyclists' comfort zones from obstacle avoidance manoeuvres. *Accident Analysis & Prevention, 144* 105609.

Lubbe, N. (2017). Brake reactions of distracted drivers to pedestrian Forward Collision Warning systems. *Journal of Safety Research, 61*, 23–32.

Svärd, M., Markkula, G., Engström, J., Granum, F., & Bärgman, J. (2017). A quantitative driver model of pre-crash brake onset and control. In *Proceedings of the human factors and ergonomics society annual meeting* (Vol. 61, No. 1, pp. 339-343). Sage CA: Los Angeles, CA: SAGE Publications.

Vella, A. D., & Vigliani, A. (2022). Research on the longitudinal dynamics of an electric scooter. *SAE International Journal of Vehicle Dynamics, Stability, and NVH*, 7(10-07-01-0003).

Vetturi, D., Tiboni, M., Maternini, G., Barabino, B., & Ventura, R. (2023). Kinematic performance of micro-mobility vehicles during braking: experimental analysis and comparison between e-kick scooters and bikes. *Transportation research procedia, 69*, 408–415.

Viviani, P., & Flash, T. (1995). Minimum-jerk, two-thirds power law, and isochrony: converging approaches to movement planning. *Journal of Experimental Psychology: Human Perception and Performance, 21*(1), 32.

Wada, T., Doi, S. I., Tsuru, N., Isaji, K., & Kaneko, H. (2010). Characterization of expert drivers' last-second braking and its application to a collision avoidance system. *IEEE Transactions on Intelligent Transportation Systems, 11*(2), 413–422.

Tianyou Li received the B.E. degree in automation from Huazhong University of Science and Technology, Wuhan, China, in 2019, and the M.Sc. degree in interactive media technology from the KTH Royal Institute of Technology, Stockholm, Sweden, in 2021. Tianyou is currently pursuing the Ph.D. degree on computational models for driver behaviour in interaction with cyclists and e-scooterists, mainly in intersection scenarios. The goal of his research is to develop driver models that can improve advanced driver assistance systems and to inform the design of relevant safety test.

Jordanka Kovaceva is a researcher at Chalmers University of Technology, the Division of Vehicle Safety since 2015. She has experience in developing methods for analyses of traffic safety by using real world crash and naturalistic driving data. Her current interests include development of methods to support the design and evaluation of active safety by including behavioural models for interaction among road-users.

Marco Dozza received the Ph.D. degree in bioengineering from the University of Bologna, Italy, in collaboration with Oregon Health & Science University, Portland, OR, USA, in 2007. After graduation, he worked as a System Developer with Volvo Technology, for over two years, a research and innovation company inside the Volvo group. Since 2009, he has been with the Chalmers University of Technology, Gothenburg, Sweden, where he is currently a Professor and leads the Crash Analysis and Prevention Unit. He is an Examiner for the course Active Safety in the Master's Programme for Automotive Engineering. He is working with SAFER, the Vehicle and Traffic Safety Center at Chalmers.